

Ultrasensitive detection of biomolecules with fluorescent dye-doped nanoparticles

Wei Lian^a, Sally A. Litherland^b, Hassan Badrane^a, Weihong Tan^c, Donghai Wu^d,
Henry V. Baker^a, Paul A. Gulig^a, Daniel V. Lim^e, Shouguang Jin^{a,*}

^a Department of Molecular Genetics and Microbiology, University of Florida, Gainesville, FL 32610, USA

^b Department of Pathology, Immunology and Laboratory Medicine, University of Florida, Gainesville, FL 32610, USA

^c Department of Chemistry, University of Florida, Gainesville, FL 32610, USA

^d Guangzhou Institute of Biomedicine and Health, Chinese Academy of Sciences, Guangzhou, China

^e Department of Biology and Center for Biological Defense, University of South Florida, Tampa, FL 33620, USA

Received 11 May 2004

Abstract

Fluorescent-labeled molecules have been used extensively for a wide range of applications in biological detection and diagnosis. A new form of highly luminescent and photostable nanoparticles was generated by doping the fluorescent dye tris(2′2-bipyridyl)dichlororuthenium(II)hexahydrate (Rubpy) inside silica material. Because thousands of fluorescent dye molecules are encapsulated in the silica matrix that also serves to protect Rubpy dye from photodamaging oxidation, the Rubpy-dye-doped nanoparticles are extremely bright and photostable. We have used these nanoparticles successfully in various fluorescence labeling techniques, including fluorescent-linked immunosorbent assay, immunocytochemistry, immunohistochemistry, DNA microarray, and protein microarray. By combining the high-intensity luminescent nanoparticles with the specificity of antibody-mediated recognition, ultrasensitive target detection has been achieved. In all cases, assay results clearly demonstrated the superiority of the nanoparticles over organic fluorescent dye molecules and quantum dots in probe labeling for sensitive target detection. These results demonstrate the potential to apply these newly developed fluorescent nanoparticles in various biodetection systems.

© 2004 Elsevier Inc. All rights reserved.

Fashionable fluorescence techniques have changed the face of today's science and technology. Fluorescent labeling techniques have been used extensively in both biological research and clinical diagnosis. To achieve sensitive detections, there is an increasing demand for fluorescent labeling probes that are more intense and stable. The traditional fluorophores such as FITC¹ are

not photostable in addition to the problem of relatively low fluorescence intensity [1–3]. Although the new generation of fluorophores such as the Alexa series have dramatically increased the labeling efficiencies, the molecular nature of the dyes determines the limitations in fluorescence intensity and photostability. Because of the advanced computational technologies and the difficult

* Corresponding author. Fax: +1 352 392 3133.

E-mail address: sjin@mgm.ufl.edu (S. Jin).

¹ Abbreviations used: FITC, fluorescein isothiocyanate; FLISA, fluorescent-linked immunosorbent assay; TEOS, tetraethylorthosilicate; NP, nanoparticle; NHS, N-hydroxysuccinimide; DETA, trimethoxysilylpropyldiethylenetriamine; PE, phycoerythrin; SEM, scanning electron microscope; TEM, transmission electron microscope; BSA, bovine serum albumin; PBS, phosphate-buffered saline; PBMC, peripheral blood mononuclear cells; DAPI, 4′,6-diamido-2-phenylindole dihydrochloride; ChAT, choline acetyltransferase; F.I., fluorescence intensity; QD, quantum dots; ELISA, enzyme-linked immunosorbent assay; Ab, antibody; Ag, antigen.

biological problems of detecting low-abundance targets, the demand for revolutionary fluorescence technologies is unprecedented.

Advances in the development of semiconductor nanocrystals (quantum dots) opened a promising field in the development of a new generation of luminescent biomarkers [4,5]. These luminescent dots have been functionalized to couple biomolecules [6–8]. Recent reports described the successful application of this labeling agent in immunocytochemistry and immunohistochemistry and demonstrated that these markers are better labeling agents than commonly used organic dye molecules [9,10]. The commercialization of quantum dots is expected to facilitate the utilization of this new form of biomarker in various applications. Although the replacement of traditional dyes will be a slow process, an age of more variety in labeling is just a matter of time [11–13].

Santra et al. [14] have developed a dye-doped nanoparticle (NP) technology which encapsulates many thousands of dye molecules inside silica nanoparticles and thus has the following advantages: (i) high intensity of the fluorescent signal, (ii) excellent photostability due to exclusion of oxygen by silica encapsulation, (iii) efficient conjugation with various biomolecules due to the silica surface which is simple to modify, and (iv) easy manufacturing process. The highly luminescent and photostable nanoparticles were generated by doping a luminescent dye, tris(2,2'-bipyridyl)dichlororuthenium (II) hexahydrate (Rubpy), into a silica matrix [14]. The nanoparticles contain a large number of dye molecules, which form the foundation for luminescence detection with significant signal amplification. The nanoparticles can be made in uniform sizes, with diameters from a few nanometers to a few micrometers, and the size distribution can be controlled within 2% [14]. The silica coating prevents photobleaching by effectively excluding oxygen; thus the dye molecules within the nanoparticles are photostable. In addition, silica surface has been demonstrated to be an excellent substrate suitable for many surface immobilization mechanisms. The silica surface also aids in the dispersion of the nanoparticles in aqueous solution; thus it is highly "soluble" in aqueous solution. This property makes it suitable for application in solution-based bioassays.

In this report, we describe the application of these newly developed dye-doped nanoparticles coupled with antibodies for sensitive detection of antigens using various formats, including fluorescent-linked immunosorbent assay (FLISA), immunocytochemistry, immunohistochemistry, and DNA and protein microarrays. Compared with conventional fluorescent labeling which is based on single molecules, the bioconjugated nanoparticles that gather thousands of dye molecules in each particle are extremely bright. Our results clearly demonstrate the superiority of such nanoparticles over the existing fluorescent labeling agents, including quantum

dots. Successful utilization of the fluorescent nanoparticles in such a variety of applications clearly demonstrated their potential to be used in various bioassay systems for ultrasensitive detection.

Materials and methods

Materials

Tris(2,2'-bipyridyl)dichlororuthenium(II)hexahydrate, tetraethylorthosilicate (TEOS), Triton X-100, *n*-hexanol, cyclohexane, ammonium hydroxide (NH₄OH; 28–30 wt.%), succinic anhydride, 1-ethyl-3-(3-dimethylaminopropyl)carbodiimide hydrochloride, and *N*-hydroxysuccinimide (NHS), human IgG (hIgG), goat anti-hIgG, goat anti-mouse IgG, goat anti-mouse IgG-alkaline phosphatase, avidin, and streptavidin were purchased from Sigma/Aldrich Chemical (St. Louis, MO). Trimethoxysilylpropyldiethylenetriamine (DETA) was purchased from United Chemical Technologies (Bristol, PA). QD 605 was purchased from Quantum Dot (Hayward, CA). Avidin-conjugated Texas red, streptavidin-conjugated FITC, and streptavidin-conjugated phycoerythrin (PE) were purchased from Molecular Probes (Eugene, OR). Monoclonal mouse anti-hIgM, anti-CD3, and isotype mouse IgG (mIgG) antibodies were purchased from BD Biosciences (Bedford, MA).

Synthesis of dye-doped nanoparticles

Nanoparticles were synthesized by using a microemulsion method as described previously [14]. Briefly, the microemulsion was formed by mixing cyclohexane (7.5 ml), *n*-hexanol (1.8 ml), Triton X-100 (1.77 ml), 20 mM Rubpy dye in water (0.48 ml) and TEOS (0.1 ml). After mixing for 20 min, 60 μ l of NH₄OH was added to initiate the polymerization. The reaction was allowed to continue for 24 h. When the polymerization was complete, an equal volume of acetone was added, and the mixture was vortexed to break the microemulsion state. The solidified silica NPs were collected by centrifugation at 3000g for 10 min and washed three times with 95% ethanol. Between the washes, the NPs were dispersed by vortex and sonication. The particles were air dried and weighed for yield. Typical yield was about 20 mg. The synthesized NPs were characterized by spectrofluorometer for fluorescence intensity and by scanning electron microscope (SEM; Hitachi H FE 4000) and transmission electron microscope (TEM; Hitachi H7000) for imaging and size measurements.

Surface modification of the nanoparticles

To conjugate with biomolecules, the following surface modifications were performed on the NPs [17,25]

(www.bangslabs.com): (i) silanization with the addition of 1 mM acetic acid and 1% DETA while stirring for 30 min; (ii) carboxyl modification by adding 10% succinic anhydride in dimethylformamide under nitrogen purge and stirring for at least 6 h; (iii) 1-ethyl-3-(3-dimethylaminopropyl)carbodiimide hydrochloride and NHS chemistry by adding 1% each in 0.1 M 4-morpholineethanesulfonic acid buffer (pH 5.6) for 15–30 min; and (iv) the newly formed NHS-functionalized NPs mixed with monoclonal antibody or avidin or streptavidin at various ratios for 2–4 h at room temperature. Remaining free NHS esters were quenched by adding hydroxylamine to 50 mM, Tris-HCl, pH 7.5, to 0.5 M, and BSA to 1%. The resulting NP conjugate was stored in PBS containing 0.1% BSA at 4°C.

Direct and indirect detection of antigens on 96-well plate format

Nunc MaxSorp 96-well microtiter plates (black) were coated with a serial dilution of biotinylated hIgG (in PBS, pH 7.4) and kept at 4°C overnight. The coated plates were then washed with PBST buffer (PBS containing 0.05% Tween 20) three times, blocked with 2% BSA (w/v) for 2 h at room temperature, and washed again with PBST. Avidin-NP (0.1 mg/ml) in 0.1% BSA/PBS or other fluorescent probes with similar fluorescence intensities were then added to the sample wells. After 30 min incubation at room temperature, excess avidin-NP or other fluorescent dyes were removed thoroughly by washing five times in PBST with vigorous shaking. Then 100 µl PBS was added to each well before measuring the fluorescence intensities in a Spectrafluor microplate reader (TECAN). The filter set Ex. 430 nm/Em. 595 nm was chosen for NP, Rubpy, and QD 605 while Ex. 590 nm/Em. 635 nm was used for Texas red.

For indirect detection, serial dilutions of hIgG were coated as above, washed with PBST, and blocked with 2% BSA for 2 h. Then the plate was incubated with 10 µg/ml biotinylated goat anti-hIgG for 1 h and washed. Finally, the sample wells were probed with avidin-NP or other fluorescent labels as described above.

Immunocytochemistry

Human peripheral blood mononuclear cells (PBMC) were purified from fresh human blood by gently layering over a Ficoll-Hypaque (Amersham Biotech) density gradient and centrifuging at 600g for 30 min. The cells in suspension were incubated with biotinylated anti-IgM monoclonal antibody (BD Biosciences) in 1× PBS (Cellgro) containing 1% BSA (Sigma) and 0.1% Na azide (Sigma) for 1 h, followed by probing with streptavidin-conjugated NP for 30 min. An aliquot of each cell suspension was applied to slides by cytospin centrifugation (600g, 4 min). Nuclear chromatin of the cells was

counterstained with DAPI (Sigma). The slides were coverslipped using aqueous GelMount with antifade (BioMedia) and analyzed using deconvolution microscopy on a Delta Vision Olympus OMT inverted fluorescent microscope and a Delta Vision deconvolution software system. Images depict three-dimensional projections of 20–0.2 µm optical slices through the cell, center focused on the DAPI-stained chromatin in the nuclei.

Immunohistochemistry

Adult female ICR mice (20–25 g), housed under standard laboratory conditions, were used in the present study. All procedures were performed according to the NIH Guide for the Care and Use of Laboratory Animals and were approved by the IACUS committee (IACUC approved protocol B083). All efforts were made to minimize animal suffering and the number of animals used. The animals were deeply anesthetized with an overdose of sodium pentobarbital and transcardially perfused with ice-cold fixative of 4% paraformaldehyde in 0.1 M PBS, pH 7.4. Mouse brains were dissected out, fixed with 4% paraformaldehyde, treated with 30% sucrose, and cut coronally at 30 µm on a cryostat. The brain slices were soaked in PBST (0.2% Triton X-100) with gentle agitation for 1 h with buffer changes every 20 min. The slices were then blocked with 2% BSA for 30 min and probed overnight with goat anti-ChAT (Chemicon International) in blocking buffer. Unbound antibodies were washed away with blocking buffer. The slices were stained with 10 µg/ml streptavidin-NP in blocking buffer and counterstained with DAPI for 15 min. The slides were washed three times with PBST and mounted with 90% glycerin for observation under fluorescent microscope.

DNA microarray

Genomic DNA from *Pseudomonas aeruginosa* was prepared using the Wizard Genomic DNA Purification kit (Promega) followed by DNase I limited digestion. The digested DNA was extracted with phenol/chloroform, precipitated with ethanol, and resuspended in water. Dilutions of the DNA were made in 50% dimethyl sulfoxide and printed on CMT-GAPS slides (Corning) by using MicroCaster Handheld Arrayer (Schleicher & Schuell BioSciences). The slides were processed following the instructions from Corning Microarray Technology. Biotinylation of DNA probes was made using the BioPrime DNA Labeling System (Invitrogen). The hybridization reaction was conducted in 4× standard saline citrate + 0.1% SDS at 55°C overnight in a hybridization chamber. Posthybridization washes were performed according to the instruction manual. Posthybridization labeling was done by adding avidin-NP or streptavidin-Cy3 (0.1 mg/ml each in 10 mg/ml

BSA/PBS) to the slide and shaking for 30 min at room temperature (in the dark). The slides were finally washed with 200 ml PBST for 5 min, rinsed with water briefly, and dried with blowing air. The slides were scanned and data were processed by GenePix 4000B scanner and GenePix Pro 3.0 software (Axon Instruments).

Protein microarray

Serial dilutions of biotinylated hIgG were made in PBS containing 40% glycerin. Samples were manually spotted onto SuperEpoxy substrate (Erie Scientific) using MicroCaster Handheld Arrayer. For each concentration, at least four replica spots were printed. The printed slides were kept at room temperature overnight and treated with blocking buffer (1% BSA in PBS) for 2 h to block the active epoxy groups. About 0.4 ml of avidin-NP (0.2 mg/ml) in blocking buffer was added to each slide; the slides were then incubated for 30 min at 4 °C. To wash away the excess avidin-NP, the slides were put in 200 ml PBST in a glass tank with slide holders and shaken for 30 min at room temperature. The slides were then rinsed with water and dried. The protein chip data were collected and processed by GenePix 4000B scanner and GenePix Pro 3.0 software (Axon Instruments).

For the sandwich array, 0.5 mg/ml capture antibodies (goat anti-hIgG or goat anti-mIgG) was printed on SuperEpoxy slides. The printed slides were kept at room temperature and blocked as stated above. Various amounts of hIgG or mIgG were added to the blocks and the slides were incubated for at least 4 h at 4 °C. Excess “antigen” was washed away and the slides were incubated with 10 µg/ml biotin-labeled goat anti-hIgG or goat anti-mIgG for 2–5 h. To reduce the background, the slides were blocked one more time with 1% BSA/PBS for 30 min and then labeled with 0.2 mg/ml avidin-NP, suspended in 1% BSA/PBS for 15 min, and washed with PBST three times, 5 min each time. Finally, the slides were rinsed with water, spun or air dried, and subjected to scanning and analysis as described above.

Results

Fluorescent intensity and photostability of the Rubpy-doped silica nanoparticles

The Rubpy-doped silica nanoparticles were synthesized using a water in oil microemulsion method [14]. The NPs were prepared in multiple vials of small volume (11.7 ml) that each yielded about 20 mg of dried NP powder. The NPs from each preparation were viewed under both scanning electron microscope and transmission electron microscope to determine uniformity and the sizes of the NPs. As shown in Figs. 1A and B, the NP preparations were uniform in shape with average diameter

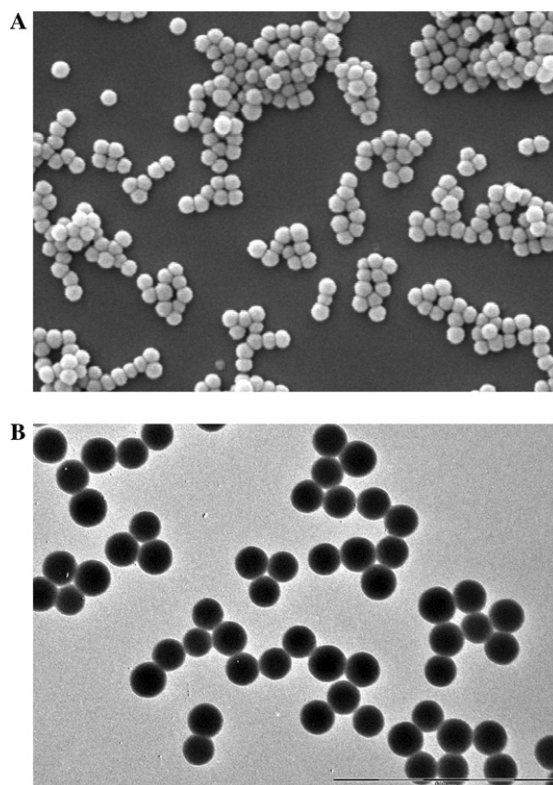


Fig. 1. Visualization of uniform-sized dye-doped nanoparticles under (A) scanning electron microscope and (B) transmission electron microscope.

of the particles around 70 nm. The absorption and fluorescence emission spectra shown in Figs. 2A and B are the same as those of the Rubpy dye used to make the nanoparticles.

Fluorescence intensity (F.I.) of the NPs was compared to that of quantum dot QD 605, Texas red, and Rubpy dye. The QD 605 is a semiconductor nanoparticle which has been reported to be extremely bright in comparison with organic dyes [9,10,15]; the Texas red is a commonly used organic dye which has the closest emission wavelength to that of NPs, whereas the Rubpy dye is the fluorescence material of which the NPs are made. Serially diluted nanoparticle and fluorescence dyes were measured for F.I. at their corresponding optimal excitation/emission wavelengths. In each case, a linear relationship between the F.I. and the concentration of the fluorescent particle/molecule was observed (data not shown). From the data, we were able to calculate the F.I. of each mole of particles or molecules and found that the F.I. of a single NP is equivalent to that of 39 particles of QD 605, 1290 molecules of Texas red, and 72,413 molecules of Rubpy dye (Table 1). Clearly, the dye-doped nanoparticles emit extremely bright fluorescent light.

The photostability of the NP was further compared against QD 605, Rubpy dye, and Texas red. QD 605 was chosen among different-sized quantum dots because it has the same emission wavelength as that of Rubpy NP.

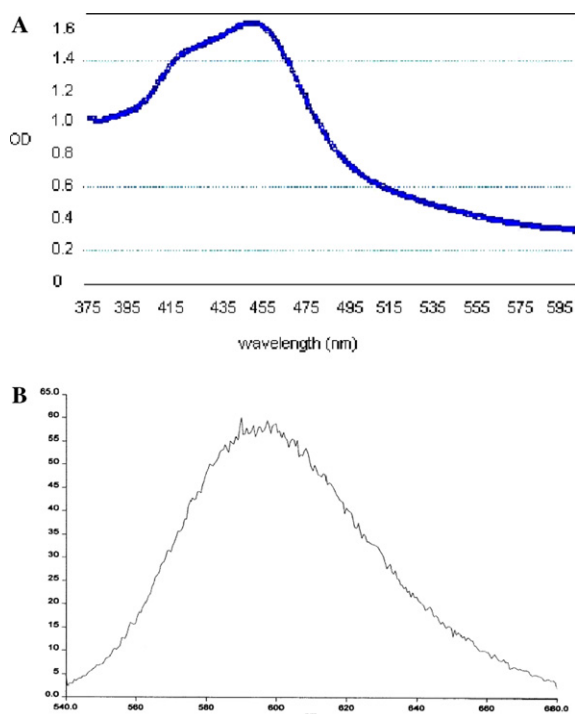


Fig. 2. Absorption spectrum (A) and emission spectrum upon excitation at 450 nm (B) of the Rubpy-doped nanoparticle.

Table 1
Comparison of fluorescence intensities of various labeling agents

	Ex./Em. wavelengths (nm/nm)	F.I. per mole	Molar ratio
NP	430/595	6.3×10^{12}	1
OD605	430/595	1.6×10^{11}	39
Texas red	590/635	4.88×10^9	1,290
Rubpy	430/595	8.7×10^7	72,413

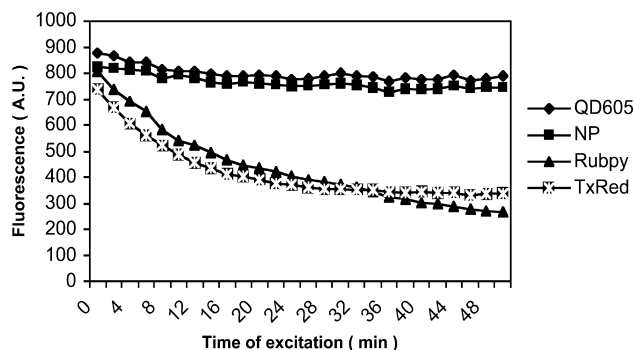


Fig. 3. Comparison of photostability of the dye-doped nanoparticle, quantum dot (QD 605), Texas red, and Rubpy dye molecules. Liquid solutions containing similar fluorescent intensities were exposed to 50-W light under respective optimal excitation wavelengths and fluorescent intensities were measured at 2-min intervals.

Each fluorescent agent was excited continuously at its optimal excitation for 50 min using Spectrafluor microplate reader (TECAN), and the fluorescence intensity was measured every 2 min. The results shown in Fig. 3 clearly demonstrate that the NP is as stable as the QD

and both are much more stable than Texas red and Rubpy dye.

Efficient conjugation of NPs with biomolecules

Biomolecules such as antibodies and enzymes can easily be conjugated to the silica surfaces of NPs. Using the established method [16,17], the NPs were successfully conjugated with antibodies, streptavidin, or avidin. To monitor the conjugation efficiency, a fixed amount of functionalized NPs was conjugated with varying amounts of mouse anti-hIgG (see Materials and methods). Upon completion of the conjugation, NPs were completely precipitated by ultracentrifugation and the supernatant was used to conduct quantitative ELISA to detect the amount of unconjugated Ab. The ELISA involved coating 96-well plates with hIgG, binding with the Ab in the supernatant of the conjugation reaction, and detecting with alkaline-phosphatase-conjugated goat anti-mIgG. A standard curve using serial dilutions of known amounts of mouse anti-hIgG was generated. Under the assay condition, the conjugation rate was close to 100% when the ratios of Ab to NP were at 50:1, 100:1, and 200:1 (data not shown), suggesting that each NP can efficiently conjugate at least 200 molecules of Ab. Using antibodies against avidin and streptavidin, each NP was also determined to be able to conjugate at least 200 molecules of avidin or streptavidin with almost 100% efficiency (data not shown).

Application of the NPs to fluorescence-linked immunosorbent assay

This assay system is identical to that of ELISA except that fluorescent NP takes the place of enzyme. Biotinylated hIgG along with regular hIgG were immobilized on 96-well microtiter plates in serial dilutions. The coated plates were blocked with BSA and probed with avidin-conjugated NP. After unbound avidin-NP was washed away, the fluorescence intensities were measured. Results shown in Fig. 4A indicated a highly specific binding of the avidin-NP to the hIgG-biotin. The relationship between the fluorescence intensity and the hIgG-biotin concentration was linear in the range from 20 ng/ml to 2.5 mg/ml. This assay is fast, easy, highly reproducible, and thus applicable to detection and quantitation of any biotinylated substrates.

To investigate the practical advantage of using NPs, the NPs were compared in parallel with QDs and Texas red in the otherwise identical FLISA. All the avidin-conjugated fluorescent probes were adjusted to have the same fluorescence intensity (~ 4000 A.U.) before probing. Each fluorescent probe was incubated with the target for 30 min at room temperature. After washes, the fluorescence intensities were measured at corresponding optimal Ex/Em wavelengths. Again, the NP is a superior

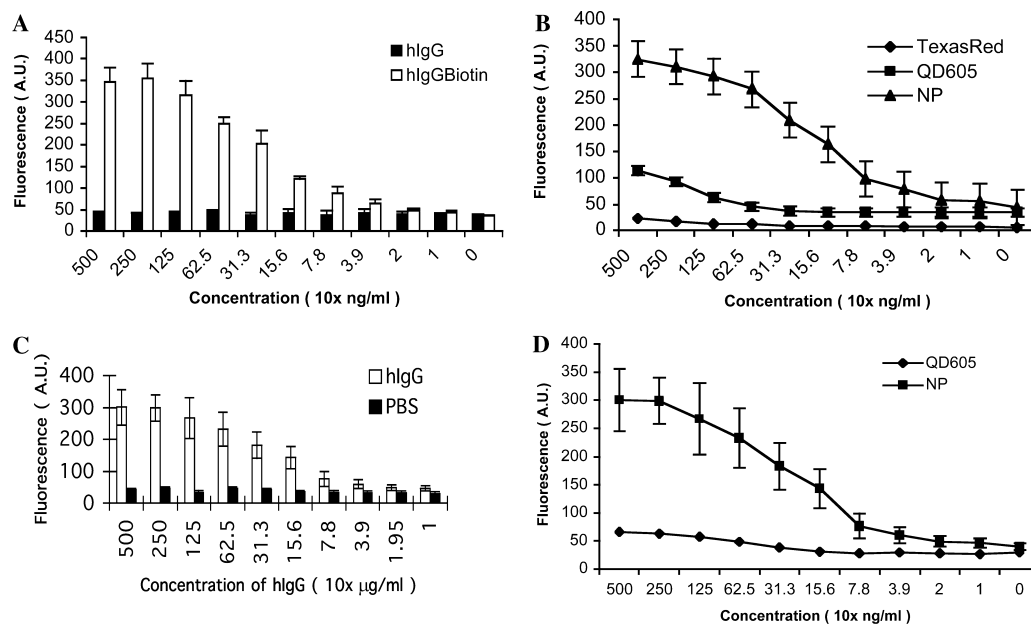


Fig. 4. (A) Comparison of fluorescent signal intensities in 96-well plates that were coated with varying concentrations of hIgG-biotin or hIgG and developed with the avidin-NP. (B) Comparison of fluorescent signal intensities detecting the same amount of antigens by avidin-conjugated NP, QD 605, and Texas red. (C) Fluorescent signal intensities for detecting varying amounts of hIgG using an indirect FLISA where plates were coated with varying concentrations of hIgG first and then detected with biotin-labeled goat anti-hIgG followed by avidin-NP. (D) Comparison of antigen detection sensitivities between the use of avidin-conjugated NP and QD 605 in the indirect FLISA.

labeling agent (Fig. 4B). Under our assay condition, the target detection limits (average of negative control + $3 \times$ SD) were 1.9, 62.5 and 250 ng for NP, QD, and Texas red, respectively (data not shown).

In most cases, it is either inconvenient or impossible to biotinylate the biological target molecules; therefore, an indirect FLISA has been tested. In this particular experiment, 96-well plates were coated with a serial dilution of hIgG, probed with biotinylated goat anti-hIgG antibody, and then detected with avidin-conjugated NP (Fig. 4C). Similar to the above direct FLISA, the fluorescence intensity was in linear relationship with the concentration of the hIgG; thus this assay can be used to detect and quantify any biological targets. Once again, taking advantage of the assay system, we compared the NP and QD 605 for signal amplification in target recognition. As shown in Fig. 4D, for a given amount of target, NP labeling can give rise to much stronger signal than that by QD 605 and the detection sensitivity by NP is about 50-fold higher than that by QD 605.

NP-mediated labeling of target molecules on cells and tissues

We investigated the application of NPs in the areas where traditional fluorescent dyes are used. The most widely used technique with the fluorescent dyes is probably fluorescent microscopy. If we are able to use NPs to specifically label cells and tissue sections, the combined characteristics of sensitivity and photostability can potentially make the NPs a superior labeling tool.

We first applied NPs in the research area of immunocytochemistry. Immunolabeling of cell surface markers is commonly used in cell biology, immunology, and clinical laboratories. IgM is a surface marker of certain populations of lymphocytes (B cells); we tested the ability to label IgM-positive lymphocytes by using biotinylated anti-IgM and streptavidin-conjugated NP. Lymphocytes can easily be distinguished from monocytes and macrophages by morphological observation under the microscope. Human peripheral blood mononuclear cells were purified from fresh blood donated by volunteers (see Materials and methods). The purified PBMC were incubated with biotinylated anti-IgM monoclonal antibody (BD Biosciences) and streptavidin-conjugated NP in suspension. After washing away unbound antibody and NP, the cells were applied to slides by cytospin centrifugation. The nuclear chromatin were then counterstained with DAPI (Sigma). The IgM-bearing cell surfaces were labeled with NPs which emit red fluorescence while all the cellular nuclei were stained by DAPI which emits blue fluorescence (Fig. 5A). Combined with the cell morphology, the NPs specifically labeled B cells and the stains were localized on one part of the cell surface, due to what is known as antigen capping [18–20]. Similar cell surface labeling was observed when conventional organic dye PE was used, but with much weaker labeling intensity (Fig. 5A). Clearly, the NPs can mediate specific labeling of B cell surface IgM molecules.

We further extended the application of NPs in the area of immunohistochemistry. As with blood or cultured cells, tissue sections are also routinely labeled

with fluorescent dyes in both research and clinical laboratories. For example, in the brain of Alzheimer's patients, cholinergic neurons in the basal forebrain area are often reduced or depleted [21]. Therefore, specific labeling of cholinergic neurons is an important tool in both clinics and research of Alzheimer's disease. Choline acetyltransferase is a cytoplasmic protein which exists only in the cholinergic neurons in the brain, such that ChAT is by far the best known cholinergic marker [22,23]. We used affinity-purified polyclonal antibodies against ChAT (Chemicon International) to probe the cholinergic neurons in the brain. Mouse brain tissue sections were incubated with biotinylated goat anti-ChAT antibodies, followed by labeling with streptavidin-conjugated NP and DAPI (Fig. 5B). The nuclei of all cells were stained by DAPI which marked the whole cell population (neurons and glial cells). The cell bodies of selected neurons were also stained by NPs which are characteristic cholinergic neurons judged from the morphology and localization of the NP-stained cells [22,23].

Use of the NPs in DNA microarray detection

In recent years, high-throughput technologies, such as microarrays, have changed the ways that researchers

approach biological problems. DNA microarrays have been widely used in genomics, drug discovery, and clinical diagnosis. However, accurate detection of low-abundance targets is still the biggest challenge. Therefore, we investigated the application of NPs to DNA microarrays, hoping to add a new tool to the tool box of the chips technology.

Using MicroCaster Handheld Arrayer (Schleicher & Schuell BioSciences), genomic DNA from *P. aeruginosa* was manually printed on the CMT-GAPS slide (Corning) which was thereafter processed according to the manufacture's instruction. The slide was probed by biotinylated *P. aeruginosa* DNA and then by avidin-conjugated NP or streptavidin-conjugated Cy3. To begin, we printed the same amount of DNA in each spot to determine the consistency of the staining in comparison with Cy3. Fig. 6A shows two clusters of arrayed DNA of the same concentration (100 $\mu\text{g}/\text{ml}$) with the top block labeled with NP and the bottom block labeled with Cy3. Under the same condition, the DNA array labeled with NP was much brighter than that with Cy3. It should be noted that the fluorescent signals were scanned using the optimal Ex/Em wavelength for the Cy3 due to the lack of that for NP, at which the NP emits only 5% of its maximum. These data indicate that NP is applicable to

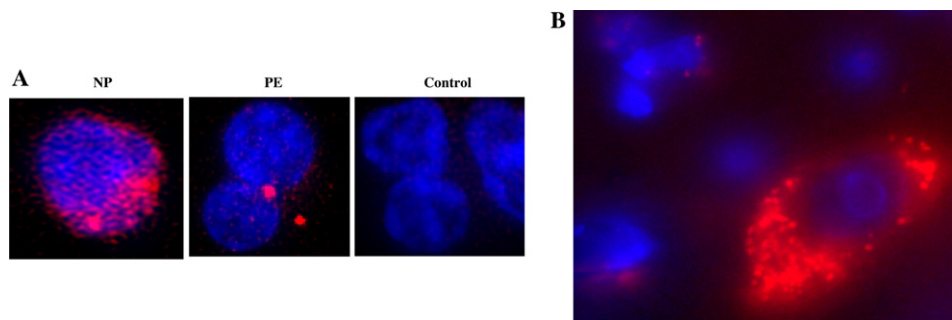


Fig. 5. (A) Labeling of B cell surface IgM molecules with NP and PE. Human peripheral blood mononuclear cells (PBMC) were first incubated with biotinylated mouse anti-hIgM and then with avidin-NP or avidin-PE (red). The PBMC were also stained with DAPI to visualize the nuclei (blue). (B). Labeling of choline acetyltransferase (ChAT) using NP. Mouse brain section was first incubated with biotinylated goat anti-ChAT Ab and then detected with avidin-NP (red). Cells were also stained with DAPI (blue). (For interpretation of the references to colour in this figure legend, the reader is referred to the web version of this paper.)

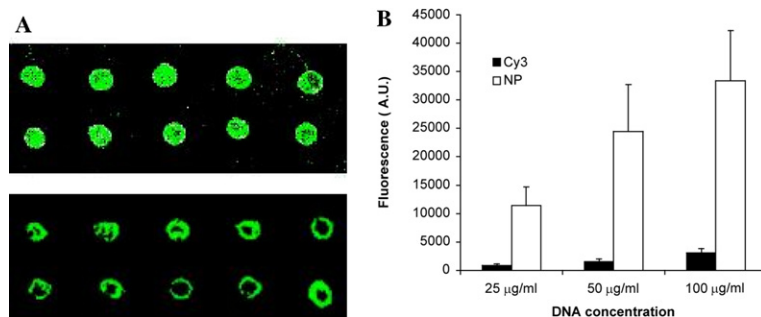


Fig. 6. Labeling of DNA microarray with NP or Cy3. (A) DNA chips spotted with the same amount of *Pseudomonas aeruginosa* genomic DNA were hybridized with biotinylated probes generated from *P. aeruginosa* genomic DNA and detected with either avidin-labeled NP (upper slide) or Cy3 (lower slide). The images were scanned with optimal excitation and emission wavelengths for Cy3. (B) Quantitative detection of target DNA on the microarray with avidin-NP (white bar) or with Cy3 (black bar) after scanning under optimal excitation and emission wavelengths for Cy3.

DNA microarray labeling and is superior to traditional fluorescent dye Cy3. Furthermore, due to the high fluorescence intensity, the NP can potentially be used for detection of low-abundance targets.

To investigate whether there is correlation between the amount of DNA spotted and the signal intensity, the arrays were printed with different DNA concentrations. As shown in Fig. 6B, the detected fluorescence signals did reflect the amount of DNA on the array, suggesting that the NP-mediated target detection can be used for quantitation.

Use of the NPs in protein microarray detection

Protein microarrays have great potentials in global studies of protein expression, protein profiling, and protein–protein interactions among others. It has become an increasingly important tool in functional genomics and proteomics. We initially examined the direct labeling format in protein microarray detection. Human IgG-biotin along with regular hIgG was manually spotted on SuperEpoxy microarray slides (Erie Scientific). For both samples, 1:2 serial dilutions were made starting from the concentration of 0.5 mg/ml down to 100 ng/ml and spot-

ted in the order from left to right. After blocking with 1% BSA, the slides were labeled with avidin-NP and scanned using GenePix 4000B scanner (see Materials and methods). As shown in Fig. 7A, there were strong signals in the upper four rows where hIgG-biotin was spotted, while no signal was detected in the lower four rows where hIgG was spotted (negative controls), indicating a high labeling specificity. Also, the fluorescence intensity from each spot was in proportion to the concentration of hIgG-biotin applied, demonstrating the possibility to quantify the amount of target by measuring the fluorescence.

To compare the sensitivity with conventional organic dyes, two identical hybridizations have been carried out on slides, one labeled with FITC and the other with NP. The fluorescent signal intensities of the spots were analyzed using optical image analysis technology due to the lack of excitation/emission wavelengths optimal for the FITC and NP in the GenePix 4000B scanner. Pictures of both the NPs and the FITC-stained spots were taken using the fluorescent morphometric microscope and Hamamatsu low-light fluorescent digital camera (Imaging Research). The brightness of the spots labeled with NP and FITC were compared using the

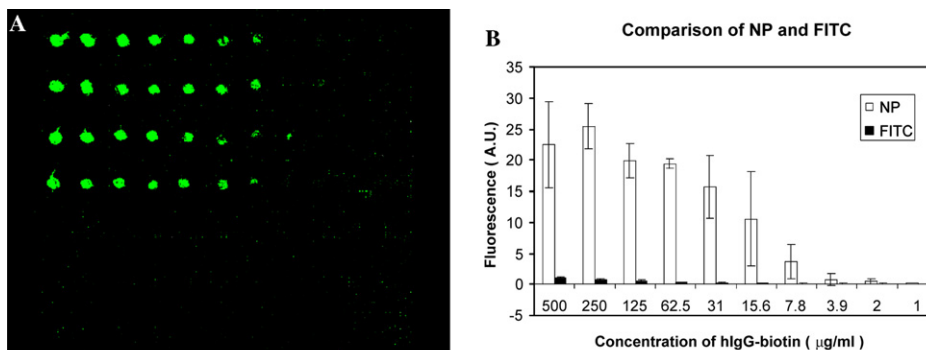


Fig. 7. Labeling of protein chips with the NP or FITC. (A) Top four rows were spotted with serial dilution (from left to right) of biotinylated hIgG while lower four rows were spotted with that of hIgG. Avidin-NP was used to detect the fluorescence. (B) Comparison of fluorescent signal intensities of protein chips labeled with either NP or FITC.

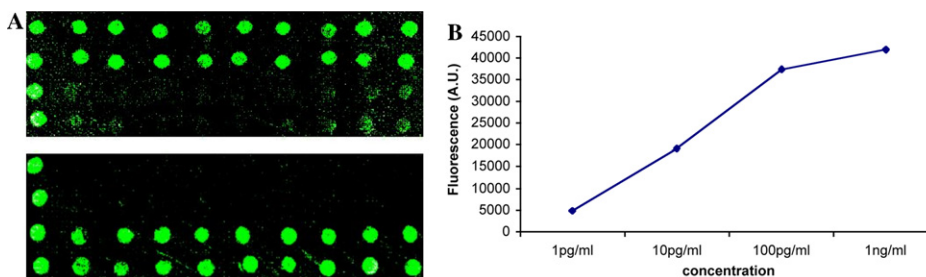


Fig. 8. Microarray detection of hIgG and mIgG. (A) Two identical slides spotted with goat anti-hIgG on upper two rows and goat anti-mIgG on lower two rows. First column on the left was spotted with biotinylated hIgG as positive control. Top slide was incubated with hIgG and biotinylated goat anti-hIgG while the bottom slide was incubated with mIgG and biotinylated goat anti-mIgG. Both slides were labeled with avidin-NP for fluorescent signal detection. (B) Detection of various concentrations of mIgG as antigen. Slides spotted with goat anti-mIgG were hybridized with varying concentrations of mIgG and detected with excess of biotinylated goat anti-mIgG followed by avidin-NP. The signal intensities of the slides were normalized using the positive control spots (hIgG-biotin). Average signal intensities were plotted against the concentrations of mIgG used in the hybridization.

MicroComputer Imaging Device software. Analysis results showed that the microarrays labeled by NP are about 80 times as bright as those by FITC (Fig. 7B).

We further performed sandwich microarray to detect human IgG and mouse IgG. The capture antibodies, goat anti-hIgG and goat anti-mIgG, were each printed in two repeating rows on the slides. As positive control, biotinylated goat anti-hIgG was spotted at the beginning of each row. As shown in Fig. 8A, the top slide was incubated with hIgG as antigen and biotinylated goat anti-hIgG as detection antibody, while the bottom slide was incubated with mIgG as antigen and goat anti-mIgG-biotin as detection antibody. Both slides were then labeled with avidin-NP. The results demonstrated a high detection specificity, as there were little cross-labeling between hIgG and mIgG. Next, the identical array slides were incubated with varying concentrations of mIgG (1:10 serial dilutions) and detected with goat-anti-mIgG-biotin followed by labeling with avidin-NP. The signal intensities were normalized using the positive control spots (goat anti-hIgG-biotin) and the fluorescent signal intensities were compared. As shown in Fig. 8B, the fluorescent signal intensities were proportional to the concentrations of the antigen (mIgG), with a detection limit of below 1 pg/ml; thus the NPs are applicable to the quantitative analysis of the protein microarrays.

Discussion

Nanomaterials have demonstrated their unique advantages when they are combined with biomolecules for bioanalysis and biotechnology applications [24]. The demand for highly sensitive nonisotopic bioanalysis systems for biotechnology applications such as in clinical diagnostics, food quality control, drug delivery, etc. has driven nanomaterials more toward biomedical fields and biotechnology. The novel nanoparticles described in this report can each emit an extremely strong fluorescent signal, enabling us to achieve enormous signal amplification for ultrasensitive target detection and for monitoring rare events that are otherwise undetectable with the existing labeling technologies. Furthermore, the nanoscale size of the particles minimized physical interference with the biological recognition events, while the nature of silica particles enables us to easily modify their surfaces for conjugation with various biomolecules for a wide range of applications in bioassay systems. Moreover, the potential to prepare the nanoparticles with any existing fluorophores provides the diversity of nanoparticles for various applications.

In this study, we demonstrated the utility of the dyed nanoparticles in ultrasensitive bioanalysis by adapting to the existing assay systems. Compared to conventional immunoassays, where an antibody-antigen binding event brings only a few dye molecules for signal-

ing, the bioconjugated nanoparticles enable significant amplification of the analytical signal due to the many dye molecules inside each nanoparticle. Apparently, the size of the nanoparticle does not seem to affect the antigen-antibody binding specificity as seen from comparison of labeling efficiency in NP and conventional organic dyes, such as Texas red, FITC, and PE (Figs. 4 and 5).

Based on the results of the fluorescent-linked immunosorbent assay, the nanoparticles can generate specific and high-intensity fluorescent signals according to the Ag-Ab interaction, thus making real-time detection of the bacterial or viral pathogens a possibility. The dyed nanoparticles are hundreds of times smaller than bacteria; thus by conjugating the nanoparticles with antibodies that specifically recognize the bacterial surface antigens (lipopolysaccharides), as high as 10^4 nanoparticles can bind to the surface of each bacterial cell. Such high numbers of surface-bound nanoparticles should generate sufficient fluorescent signal for detection, achieving ultrasensitive detection of bacterial cells. Furthermore, since it does not require any amplification step, the bacterial detection process can be adopted to real-time detection.

Immunofluorescent labeling of both cell surface marker and tissue sections also demonstrated high specificity and high intensity, thus making a direct observation for instant diagnosis of pathological samples in surgery rooms a possibility. Identifying rare and low-abundance disease markers quickly with simple procedures is a tremendous challenge in clinical pathology. For instance, during surgical removal of diseased tissues, a real-time diagnosis of the removed tissues for the presence of disease markers will be a tremendous advantage for making on-site decision for complete or partial removal of the diseased tissues. The nanoparticle-mediated simple and sensitive detection might provide such procedure.

The expanding knowledge of the genome and its macromolecular products (RNA, protein) reveals that diseases can be linked to specific alterations in the molecular processes of affected cells and tissues. The emerging profiles of macromolecular changes in disease are providing the substrate for the definition of molecular signatures of disease that will be useful for early detection and diagnosis and provide targets for the development of new strategies for prevention and therapy. This fundamental observation lays the foundation for new strategies to monitor the maintenance of health and the emergence of the earliest signatures of disease or genome damage and to provide specific and effective intervention. The DNA and protein chip technologies provide means for such early detection. As with most other relevant technologies, one of the outstanding issues in chip technology is how to accurately detect low-abundant targets. The problem can be solved by increasing either the detection sensitivity or

the fluorescent signals. With the high-energy confocal laser scanners in place, the detection machineries have been pushed to their limits. High-power lasers increase the signals, but they also increase the background and the photobleaching effect on the fluorescent dyes. The more sensible approach would be the use of brighter fluorescent labeling agents. Our primitive DNA and protein chip analysis using the nanoparticles demonstrated an enhanced fluorescent signal intensity and hence an increased detection sensitivity while not affecting the specificity rendered by DNA–DNA pairing or Ab–Ag interaction. Most importantly, the signal intensity is proportional to the amount of antigen or target DNA present in the detection system; thus it is applicable to quantitative analysis in the DNA and protein chip technology.

By integrating the nanotechnology into complex biological systems, we can achieve the detection and prevention of disease at the earliest stages of its development. Nanotechnology promises scientific and commercial opportunities that are virtually unimaginable at this time. The ultimate power of the fluorescent nanoparticles will emerge as a revolutionary tool for ultrasensitive detection of disease markers and infectious agents. Indeed, by using the dye-doped nanoparticles as fluorescent markers, highly sensitive target detection has been achieved, opening the possibility for the fabrication of truly smart bioprobes and biosensors.

Acknowledgments

We thank Lisa Hilliard and Xiaojun Zhao for their assistance in the nanoparticle synthesis, Fred Bennett for assistance in electron microscopy work, and the Electron Microscopy and Flow Cytometry Core laboratories of the Interdisciplinary Center for Biotechnology Research, University of Florida. This work was supported by grants from DOD (to S.J., P.G., and D.L), the Howard Hughes Medical Institute, and the NIH NIDDK KO1 DK02947 (to S.A.L).

References

- [1] M. Dyba, S.W. Hell, Photostability of a fluorescent marker under pulsed excited-state depletion through stimulated emission, *Appl. Opt.* 42 (2003) 5123–5129.
- [2] L. Galassi, Wavelength dependence of the time course of fluorescence enhancement and photobleaching during irradiation of ethidium bromide-stained nuclei, *Eur. J. Histochem.* 44 (2000) 419–432.
- [3] X. Fang, W. Tan, Imaging single fluorescent molecules at the interface of an optical fiber probe by evanescent wave excitation, *Anal. Chem.* 71 (1999) 3101–3105.
- [4] W.C. Chan et al., Luminescent quantum dots for multiplexed biological detection and imaging, *Curr. Opin. Biotechnol.* 13 (2002) 40–46.
- [5] J.L. West, N.J. Halas, Engineered nanomaterials for biophotonics applications: improving sensing, imaging, and therapeutics, *Annu. Rev. Biomed. Eng.* 5 (2003) 285–292.
- [6] M. Bruchez, M. Moronne, P. Gin, S. Weiss, A.P. Alivisatos, Semiconductor nanocrystals as fluorescent biological labels, *Science* 281 (1998) 2013–2016.
- [7] W.C. Chan, S. Nie, Quantum dot bioconjugates for ultrasensitive nonisotopic detection, *Science* 281 (1998) 2016–2018.
- [8] M. Han, X. Gao, J.Z. Su, S. Nie, Quantum-dot-tagged microbeads for multiplexed optical coding of biomolecules, *Nat. Biotechnol.* 19 (2001) 631–635.
- [9] J.K. Jaiswal, H. Mattoussi, J.M. Mauro, S.M. Simon, Long-term multiple color imaging of live cells using quantum dot bioconjugates, *Nat. Biotechnol.* 21 (2003) 47–51.
- [10] X. Wu et al., Immunofluorescent labeling of cancer marker Her2 and other cellular targets with semiconductor quantum dots, *Nat. Biotechnol.* 21 (2003) 41–46.
- [11] G. Quash et al., The preparation of latex particles with covalently bound polyamines, IgG and measles agglutinins and their use in visual agglutination tests, *J. Immunol. Methods* 22 (1978) 165–174.
- [12] D. Bourel, A. Rolland, R. Le Verge, B. Genetet, A new immunoreagent for cell labeling. CD3 monoclonal antibody covalently coupled to fluorescent polymethacrylic nanoparticles, *J. Immunol. Methods* 106 (1988) 161–167.
- [13] J. Adler, A. Jayan, C.D. Melia, A method for quantifying differential expansion within hydrating hydrophilic matrixes by tracking embedded fluorescent microspheres, *J. Pharm. Sci.* 88 (1999) 371–377.
- [14] S. Santra, K. Wang, R. Tapeç, W. Tan, Development of novel dye-doped silica nanoparticles for biomarker application, *J. Biomed. Opt.* 6 (2001) 160–166.
- [15] A. Watson, X. Wu, M. Bruchez, Lighting up cells with quantum dots, *Biotechniques* 34 (2003) 296–300.
- [16] M. Qhobosheane, S. Santra, P. Zhang, W. Tan, Biochemically functionalized silica nanoparticles, *Analyst* 126 (2001) 1274–1278.
- [17] S. Santra, P. Zhang, K. Wang, R. Tapeç, W. Tan, Conjugation of biomolecules with luminophore-doped silica nanoparticles for photostable biomarkers, *Anal. Chem.* 73 (2001) 4988–4993.
- [18] F. Loor, Ligand-induced patching and capping of surface immunoglobulins, *Methods Enzymol.* 108 (1984) 371–385.
- [19] L.S. Jugloff, J. Jongstra-Bilen, Cross-linking of the IgM receptor induces rapid translocation of IgM-associated Ig alpha, Lyn, and Syk tyrosine kinases to the membrane skeleton, *J. Immunol.* 159 (1997) 1096–1106.
- [20] M.A. Trujillo, S.W. Jiang, J.E. Tarara, N.L. Eberhardt, Clustering of the B cell receptor is not required for the apoptotic response, *DNA Cell Biol.* 22 (2003) 513–523.
- [21] Y. Oda, I. Nakanishi, The distribution of cholinergic neurons in the human central nervous system, *Histol. Histopathol.* 15 (2000) 825–834.
- [22] C.R. Houser, Cholinergic synapses in the central nervous system: studies of the immunocytochemical localization of choline acetyltransferase, *J. Electron Microsc. Tech.* 15 (1990) 2–19.
- [23] R. Quirion, Cholinergic markers in Alzheimer disease and the autoregulation of acetylcholine release, *J. Psychiatry Neurosci.* 18 (1993) 226–234.
- [24] S.A. Davis, Biomedical applications of nanotechnology—implications for drug targeting and gene therapy, *Trends Biotechnol.* 15 (1997) 217–224.
- [25] F. Kurzer, K. Douraghi-Zadeh, Advances in the chemistry of carbodiimides, *Chem. Rev.* 67 (1967) 107–152.